LANGMUIR

pubs.acs.org/Langmuir Article

# Improved Oil Recovery in Carbonates by Ultralow Concentration of Functional Molecules in Injection Water through an Increase in Interfacial Viscoelasticity

Taniya Kar, Tomás-Eduardo Chávez-Miyauchi, Abbas Firoozabadi,* and Mayur Pal

Cite This: *Langmuir* 2020, 36, 12160−12167

Read Online

ACCESS | Metrics & More | Article Recommendations

**ABSTRACT:** Injection of sea water is the most common practice to displace oil in porous media in subsurface formations. In numerous studies, conventional surfactants at concentrations in a range of one weight percent have been proposed to be added to the injected water to improve oil recovery. Surfactants accumulate at the oil−water interface and may reduce the interfacial tension by three orders of magnitude or more, resulting in higher oil recovery. Recently, we have proposed the addition of ultralow concentration of a non-ionic surfactant to the injected water to increase interface viscoelasticity as a new process. The increase in interface viscoelasticity increases oil recovery from porous media. This alternative approach requires only a concentration of 100 ppm (two orders less than the conventional improved oil recovery) and therefore is potentially a much more efficient process. In this work, we present a comprehensive report of the process in an intermediate-wet carbonate rock. There is very little adsorption of the functional molecules to the rock surface. Because the critical micelle concentration is low (around 30 ppm), most of the molecules move to the fluid−fluid interface to form molecular structures, which give rise to an increase in interface elasticity. We also demonstrate that interface elasticity has a non-monotonic behavior with the salt concentration of injected brine, and an optimum salinity exists for maximum oil recovery.

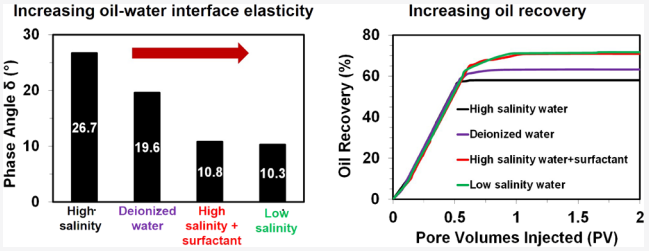


## INTRODUCTION

Injection of water in hydrocarbon formations is the most common method to increase oil recovery. The concentration and type of salt ions in the injected water may affect the efficiency of the process. A decrease in salt concentration of the injected water known as low-salinity waterflooding (LSW) may increase oil recovery.[1] LSW injection can be classified as an improved oil recovery (IOR) method, which has gained high interest over the past 10 years, with a considerable rise in literature on the subject.[2−5] Despite much research, there are various opinions on mechanisms in LSW performance. Two main parameters believed to affect the process are change in wettability toward water-wetting[6,7] and, to a less degree, the reduction of oil−brine interfacial tension (IFT). Wettability alteration depends on the type of reservoir rock; water-wet sandstones require the cationic strength of brine to be low for the repulsive forces to dominate between the rock and crude oil, leading to improved sweep. For mixed- to oil-wet carbonates, anions can induce ion exchange; the ion type is critical for the trapped oil to be released for recovery.[8,9] There are reports that LSW injection has led to high oil recovery without altering the wettability of already water-wet cores.[10] Rock−brine interactions and crude oil composition are pointed out to be the contributing factors for increased oil recovery, contrary to wettability alteration.

The effect of low salinity and deionized water on oil recovery has been explored in sandstones[11,12] and carbonates.[13] The effect of injection brine salinity on oil recovery in Berea sandstone is investigated for two different crude oils using four injection fluids—deionized water, aquifer (low salinity), seawater, and formation water.[11] Low-salinity water injection is reported to result in significant improvement in recovery by 22% compared to that of high-salinity water, and deionized (DI) water further increases recovery by 14%. This is attributed to cation exchange with the rock minerals, making the surface charge negative and reducing the electrostatic interactions with crude oil. Li[12] conducted a systematic study on the comparison of DI water and LSW performance with that of seawater in clay-bearing sandstone and found that seawater flooding should actually be considered for sandstone

**Received:** June 14, 2020
**Revised:** September 21, 2020
**Published:** September 22, 2020

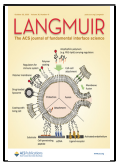







https://dx.doi.org/10.1021/acs.langmuir.0c01752
*Langmuir* 2020, 36, 12160−12167

formations containing clay since it would result in higher recovery than LSW for the same injection pressure. Clay plugging in sandstone by LSW is a very different issue compared to the process mechanisms occurring in carbonates.

Shehata et al.[13] conducted a series of waterflooding experiments on an Indiana limestone rock, with porosity, permeability, and connate water saturation of 19−20%, 160−200 mD, and 22−35%, respectively. On average, DI water injection gives a higher recovery (56.8%) compared to seawater injection (ranging from 48.7 to 50.5%) in secondary mode. Changing injection fluid from seawater to DI water and vice versa for tertiary flooding gives a significant increase in recovery. Divalent ions are reported to play a significant role in changing the surface charges, with magnesium and sulfate ions found to affect oil recovery more than calcium ions. In our work, we find a non-monotonic trend in oil recovery with change in injection brine salinity, which is different from the works reviewed above. Both monotonic and non-monotonic changes in interfacial tension of aqueous phase−crude oil systems with salt concentration have been reported in the literature. Interfacial viscoelasticity with salt concentration may also show monotonic and non-monotonic trends with salt concentration. As we will show in this work, the non-monotonic behaviors of interfacial elasticity and oil recovery are closely correlated.

In addition to LSW, surfactant addition to the injected water may increase oil recovery through a reduction of the residual oil saturation from water displacement; the process has been widely investigated.[14] The surfactants may significantly reduce the water−oil interfacial tension.[15] Often, reduction is many orders of magnitude. The concentration of surfactants in the injection water is generally in a range of 0.5−1 weight percent (wt %). The surfactants may become ineffective at very high salt concentration and temperature. We have introduced the idea of surfactant addition at ultralow concentration to increase the oil−water interfacial elasticity to reduce residual oil saturation in a preliminary work.[16] The idea has been pursued further in our recent paper.[17] This work covers a comprehensive presentation of our new process. In our understanding, the new process and low-salinity water injection are believed to be based on the same mechanism. We present the results from water injection in oil-saturated rocks at three different salt concentrations. This will allow to firmly establish the process mechanism.

Interfacial elasticity relates to the molecular structure and arrangement of molecules at the fluid−fluid interface. The elasticity of the interface can have a significant effect on how the oil front would progress during water injection in porous media. Lucassen-Reynders[18] defined interfacial rheology as the functional relation between stress, deformation, and rate of deformation in terms of coefficients of elasticity and viscosity. There may be two kinds of interfacial films—Langmuir films, in which the amphiphilic molecules are restricted only to the interface, and Gibbs monolayers, in which amphiphiles are soluble in either or both of the bulk phases but are mostly concentrated at the interface.[19] The interfacial viscoelasticity measurements are complicated because the active molecules from either of the bulk phases can move toward the interface and can change the structure/alignment, hence altering the interfacial viscoelasticity.[20] Oil−water rheology has been studied extensively in relation to the effect of asphaltenes strengthening the oil−water interface. The polar components in crude oil may lead to a rigid, highly viscoelastic oil−water interface due to the accumulation and arrangement of heavy oil components at the interface.[21−23] The process may lead to stabilization of water-in-oil emulsions at the interface.

In water displacement of oil in porous media, the effect of interfacial rheology is a relatively new idea. There have been studies highlighting the effect of viscoelasticity on the movement of oil front in water displacement of oil, leading to a more uniform interface and, consequently, higher recovery.[16,24,25] Oil−water interfacial viscoelasticity has been reported to be affected by polar components in crude oil, such as asphaltenes,[26] and types of ions in injection brine. The crude oil−water interface has been studied through micromodel experiments in low-salinity water injection in mixed-wet rocks by Emadi and Sohrabi.[27] Microemulsions of water formed at the injected water−oil interface are linked to the coalescence of water droplets at the connate water−oil interface, which improve the flowability of trapped residual oil and alteration of wettability. Garcia-Olvera and Alvarado[28] observed increased viscoelasticity and higher oil recovery by adding sulfate anions into the injected seawater in a carbonate rock. Differences in brine compositions result in comparable IFT values; however, the difference in interfacial elasticity is found to be significant and correlates to oil recovery.

Recently, Chávez-Miyauchi et al.[29] assessed the efficiency of LSW injection in Berea sandstone using five different crude oils. LSW injection improves oil recovery in some of the crudes compared to high-salinity water injection in secondary mode (continuous oil phase) but not in tertiary mode (discontinuous oil phase). There is no clear connection between oil recovery and wettability (established through contact angle) measurements. There is an increase in elastic modulus of the oil−water interface and a decrease in phase angle (representing a more elastic interface) in low-salinity brine. Additionally, a correlation is observed between oil recovery for different oils and the total base number (TBN) of the crude oils from LSW injection (compared to high-salinity water injection). It is concluded that the base constituents in the oil may adsorb at the oil−water interface, making it more elastic, resulting in increasing the oil recovery from LSW injection in secondary mode.

A very low concentration of functional molecules in the injected brine can affect the fluid−fluid interfacial viscoelasticity and improve water injection efficiency. The process may be more attractive than LSW injection if the cost of chemical is low and it is environmentally friendly. Cho et al.[17] investigated the effect of a non-ionic surfactant at a very low concentration in the injected high-salinity brine on oil recovery, compared to LSW injection, in two different carbonate rocks. The surfactant is known to prevent water-in-oil emulsion formation in the oil phase and increase oil recovery by water injection in Berea sandstone.[30] In both of the carbonate cores with vastly different porosities and pore size distributions, an increase in oil−water interfacial elasticity, indicated by a reduction in phase angle, results in higher oil recovery for seawater injection with a surfactant, compared to LSW injection. A direct relation between oil recovery and phase angle is observed.

This study is motivated by the recent works relating interfacial viscoelasticity to oil recovery. We focus on the effect of fluid−fluid and fluid−rock interactions, and a direct correlation with IOR is established. LSW may have an optimum in salt concentration in relation to an increase in oil recovery. As we will see in this work, the effect of salt concentration on oil recovery is non-monotonic. The injection


https://dx.doi.org/10.1021/acs.langmuir.0c01752
Langmuir 2020, 36, 12160−12167

of water without salt (DI water) may give a lower recovery than that of low-salinity brine. This is a first attempt to incorporate a surfactant in the aqueous phase (ranging from DI water to high-salinity water) and study the effect on IOR in terms of changes in oil−water interfacial viscoelasticity. A very low concentration at 100 ppm of a non-ionic surfactant in high-salinity brine is also injected to compare oil recovery efficiencies in Edward Yellow carbonate cores. A concern with using surfactants is the adsorption onto the rock with high adsorption being undesirable. We determine the dynamic adsorption of the surfactant on the carbonate rock through coreflow tests. We have used an intermediate-wet carbonate rock in our study. Apart from fluid−fluid interactions, ion dissolution from the rock into the brine (rock−fluid interactions) might also affect the oil−water interfacial properties. To that end, the aqueous phase is first equilibrated with the same reservoir rock used in coreflow experiments, and interfacial rheology measurements are repeated.

## MATERIALS AND METHODS

**Fluids.** The dead oil received may contain some amount of produced water in the form of water-in-oil emulsions. The oil sample was first centrifuged using a Thermo Scientific Sorvall Biofuge Primo centrifuge at 2000 rpm for 12 h. The water content was found to be less than 10 percent. The water was separated from the oil. The crude oil without water emulsions was then used for all tests. The measured properties of the crude oil are provided in Table 1. The density and viscosity of the crude oil were measured using an Anton Paar DMA5000 density meter and an Anton Paar MCR 302 Shear rheometer with 50 mm parallel plate geometry, respectively. Total acid number (TAN) and total base number (TBN) were from potentiometric titrations using 1 g of oil sample. Measurements were repeated three times, with an error range of 3%.

**Table 1. Relevant Properties of the Crude Oil**

| density at 25 °C (g/mL) | viscosity at 25 °C (cP) | asphaltene content (wt %) | total acid number ($mg_{KOH}/g$) | total base number ($mg_{KOH}/g$) |
|---|---|---|---|---|
| 0.88 | 19.8 | 2.0 | 0.1143 | 0.9689 |

Connate brine has 13 wt % salt content. Three injection brines (including DI water) of varying salinities were used in coreflows; the composition of injection brines and connate brine is provided in Table 2. The surfactant used in this work is a proprietary chemical and is denoted by DEM throughout the text. It is a non-ionic surfactant provided by CECA, France. The primary functional group of the surfactant is an ethoxylated resin.[16,30] It has a critical micelle concentration (CMC) of 30 ppm in high-salinity brine. The DEM is found to be an effective demulsifier in previous studies.[17,30] The cost of this surfactant is around of 1% of the price of the extra oil recovered.

**Table 2. Brine Composition (Weight Percent)**

| salt | connate brine | low-salinity brine | high-salinity brine |
|---|---|---|---|
| NaCl | 8.87 | 0.10 | 4.00 |
| KCl | 0.95 | | |
| $CaCl_2$ | 2.19 | | |
| $MgCl_2$ | 1.09 | | |

**Interfacial Viscoelasticity.** The storage or elastic modulus ($G'$), loss or viscous modulus ($G''$), and phase angle ($\delta$) of the crude oil−aqueous phase interface were measured by performing controlled shear deformation oscillatory tests using the Anton Paar MCR 302 rheometer via a du Noüy ring. Angular frequency and amplitude of strain were kept constant at 0.5 rad/s and 1%, respectively. All the viscoelasticity measurements were carried out for a sufficient period of time (18−24 h) and some for an even longer time to allow the storage and loss moduli to develop and stabilize. The data points were recorded at every 15 min interval. After stabilization of the curves, the final values of storage and loss moduli were reported. The phase angle was calculated based on these values. After the moduli reaches stable values, two initial measurements were further continued for 24 more hours to confirm the stability of $G'$ and $G''$.

In our study, we used phase angle as the measure of interface viscoelasticity. High phase angle is from a decrease in $G'$ and an increase in $G''$, representing the viscous nature of the interface, while low phase angle is from an increase in $G'$ and a decrease in $G''$, corresponding to an elastic interface.[16,17]

Additional interfacial viscoelasticity measurements were performed by keeping the brine in contact with the same carbonate rock, which was used for the coreflow experiments. The brine and rock were allowed to equilibrate for a period of 24 h. The purpose is to observe changes in viscoelasticity measurements due to ion dissolution from the rock into the brine, thereby altering the brine composition. This dissolution may be more pronounced for DI water compared to low salinity (LS), high salinity (HS), and connate brines (CB).

**Interfacial Tension.** IFT measurements were performed between crude oil and the aqueous phase using a Kruss Processor Tensiometer K12. A du Noüy ring was placed in the device to measure IFT. The interface was stabilized for a minimum of 2 h before the measurement. Depending on the type of crude oil and aqueous phase, the time required to reach interface equilibrium will vary. For our samples, 2 h is found sufficient to achieve equilibrium. Each run was repeated three times.

**Contact Angle.** A goniometer setup was used for measuring the water−oil contact angle. A calcite substrate was first polished using a silicon carbide film disk to have a smooth surface. Next, the substrate was immersed in the brine for 24 h. The oil droplets were then placed inversely onto the substrate and stabilized for a period of 72 h. The image of the oil droplet on the substrate, captured using a ThorLabs 12X camera, was processed by ImageJ software, and the contact angle was measured using a Drop Snake Analysis method.[31,32] Detailed description of the procedure is presented by Aslan et al.[33]

**Coreflow.** An Edward Yellow rock, with a diameter of 1.5 in and length of 6 in, was used in coreflow. The core cleaning procedure includes injection of 10 pore volume (PV) of toluene followed by injection of 10 PV of dichloromethane (DCM) and 10 PV of methanol. Next, a Soxhlet device was used for further cleaning with several cycles of toluene followed by a DCM−water mixture. Finally, the cleaned core was dried in an oven at 100 °C.

Confinement pressure was maintained at 400 psi (2.76 MPa). After porosity and permeability measurements with deionized water, the core was saturated by flowing 2−3 PV of connate brine. Then, the pressure was raised to 100 psi, and the core was aged with connate brine for 1 week. Next, the core was saturated with the crude oil, with pressure raised to 100 psi, and aged with crude oil for 3 weeks. Water injection runs were performed at room temperature and atmospheric pressure at the outlet. Water of different salt concentrations was injected in the oil-saturated rock. The effect of the functional molecule was studied by adding 100 ppm non-ionic surfactant to the injection brine after injection of around 2 PV in tests 1, 3, and 4 and from the beginning in test 2. For all the runs, the injection flow rate was maintained constant at 2 PV/day. To remove any produced water from the recovered oil, the samples were centrifuged at 2000 rpm for 8 h, and the separated oil phase was checked for remaining water presence through microscopic imaging. To examine if any water is still left in the centrifuged oil, we centrifuged again for the second time; the speed was set at 4000 rpm for a time period of 12 h, and no water was separated. The reported values of oil recovery are free of water/emulsions in the oil.

The salinity of the produced water was measured; the data show that the produced water has a salinity between that of injected water and connate water. The salinity is closer to that of connate water during the initial PV injected, and subsequently, it decreases to near the injection brine range. This is because of mixing between injection


https://dx.doi.org/10.1021/acs.langmuir.0c01752
Langmuir 2020, 36, 12160−12167

and formation brine. The low emulsion tendency of the produced water is believed to be due to the high salinity of the aqueous phase.

**Adsorption.** A Perkin Elmer Lambda XLS UV−vis Spectrometer was used to measure the concentration of the surfactant DEM in high-salinity brine after equilibration with the rock. The concentration was used to calculate the adsorption of the chemical onto the rock in the waterflow experiments. First, the brine was equilibrated for a period of 24 h with the Edward Yellow rock. The equilibrated brine was then mixed with a range of concentrations of DEM from 20 to 100 ppm, and the resulting absorbance spectrum from 220 to 300 nm wavelength was captured. There is no distinctive peak observed in the absorbance measurements in this range of wavelength; however, a slight hump is observed at 230 nm, and this wavelength was selected to measure the absorbance of the DEM in brine. Another reason for selecting 230 nm as the reference wavelength is that at higher wavelengths, the absorbance values, especially for the lower concentrations of DEM, are found to have a very low difference. The calibration plot of DEM in high-salinity brine was created.

Next, coreflow was performed with injection of 20 PV of high-salinity brine mixed with 100 ppm DEM into the Edward Yellow rock of 1.5 in diameter and 2.5 in length at a flow rate of 5 PV/day after aging the core with the high-salinity brine for 3 days. The same salt composition in brine was used for aging and injection with DEM to simplify the analysis of DEM adsorption onto the rock from the brine. The pressure drop was monitored during the run to further examine adsorption onto the rock. The produced water was collected at various intervals, and the concentration of DEM was determined using the spectrometer and the calibration plot.

## RESULTS AND DISCUSSION

In the following, we present the results from the measurement of the oil−water interface viscoelasticity, interfacial tension, and contact angle between oil, water, and rock. These results guide the understanding in relation to oil recovery performance in the flow experiments in the cores. The experiments cover preparation of the carbonate rock (core) by saturation and aging with brine and oil, then injection of brine of known composition, and measurement of the amount of produced oil at the outlet. Aging the core for a given period of time is intended to equilibrate the rock/fluid system. Before introduction of the oil in the core, equilibrium is established between the rock and the saturating brine. After oil saturation, the equilibrium is established in the rock-brine-oil system under conditions of fixed pressure and temperature. A light crude oil and brines of different salt compositions are employed, which are detailed in Table 2. An ultralow concentration of a non-ionic surfactant, which is a demulsifier (DEM), is dissolved in the brine, and the oil recovery performance with and without the surfactant is compared. We then present the adsorption of DEM onto the carbonate rock.

**Interfacial Viscoelasticity.** The oil−water interfacial viscoelasticity may affect water injection performance. An elastic interface induces smooth flow and reduces breaking off of the oil phase. The interface viscoelasticity is measured through controlled shear deformation oscillatory tests. These measurements will be linked to the water injection performance presented in the next section.

Phase angle ($\delta$) is given by the inverse tangent function ratio of viscous ($G''$) to elastic modulus ($G'$).[34] A low phase angle is representative of a more elastic fluid−fluid interface. Figure 1 presents the phase angles of the crude oil−aqueous phase interface without surfactant as well as with 100 ppm surfactant DEM in the aqueous phase. The figure shows that the interface elasticity has a minimum phase angle for LS brine (12.5°), and when the salt is above the LS concentration, there is a trend of increasing phase angle with increasing brine salinity. When DEM is added to brine, there is a significant increase in elasticity (lower phase angle) and remains fairly constant over the measured range of brine salinities. The measured $G'$, $G''$, and $\delta$ are listed in Table 3. The addition of 100 ppm DEM results in an increase in $G'$ in most of the salt concentration range, thus improving the interface elasticity. Only for the low salinity run, the change in $G'$ is not significant, which is in line with the corresponding values of $\delta$ without and with DEM.

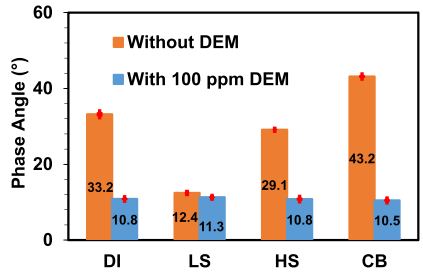


**Figure 1.** Phase angle (°) from interfacial viscoelasticity measurements of the crude oil and various aqueous phases without surfactant DEM (orange bars) and with 100 ppm surfactant DEM (blue bars): deionized (DI) water, low salinity (LS), high salinity (HS), and connate brine (CB).

To make the interfacial viscoelasticity measurements relevant to the coreflow experiments, the aqueous phase is first equilibrated with the Edward Yellow rock for a period of 24 h. There may be ion dissolution from the rock that can affect the interfacial elasticity. The measurements from Figure 1 are repeated with the rock-equilibrated aqueous phase. The comparison between the two sets of measurements is presented in Figure 2.

When the aqueous phase is equilibrated with the rock, there is a considerable change in phase angle for DI water. This is believed to be due to the dissolution of ions from the rock in the DI water, which makes the interface more elastic. However, for LS, HS, and connate brine (CB), the phase angle is slightly reduced. It should be noted that LS, HS, and CB consist of 0.1 wt % sodium chloride (NaCl), 4 wt % NaCl, and 13 wt % of a mixture of salts, respectively (Table 2). When the aqueous phase contains dissolved ions from salt, additional ion dissolution from the rock may not be significant. As a consequence, there may be no pronounced effect of equilibration of the aqueous phase with the rock on the interface viscoelasticity, Table 4 presents the data for $G'$, $G''$, and $\delta$ for the viscoelasticity measurements of brine equilibration with the rock. As we will discuss later, there is a strong relationship between the waterflow performance and interface viscoelasticity data in Table 4.

**Interfacial Tension and Contact Angle Measurements.** IFT values at room temperature without and with the 100 ppm DEM in the aqueous phase are reported in Table 5. The surfactant lowers the IFT but not significantly. We have an ongoing study on the effect of brine salinity on IFT, which shows a non-monotonic trend of oil−water IFT with salinity. There is an optimum salinity for a given oil-brine system, which results in the lowest IFT.

Table 6 shows the water−oil contact angle measurements for the crude oil with three aqueous phases. The 100 ppm DEM in the aqueous phase makes the surface slightly more water-wet, but the effect is not pronounced.



https://dx.doi.org/10.1021/acs.langmuir.0c01752
Langmuir 2020, 36, 12160−12167

Table 3. Elastic Modulus, Viscous Modulus, and Phase Angle from the Interfacial Viscoelasticity Measurements

| brine type | DEM concentration (ppm) | elastic modulus (mN/m) | viscous modulus (mN/m) | phase angle (°) |
|---|---|---|---|---|
| deionized water | | 0.138 ± 0.001 | 0.090 ± 0.002 | 33.2 ± 0.5 |
| | 100 | 0.314 ± 0.004 | 0.060 ± 0.002 | 10.8 ± 0.2 |
| low salinity | | 0.219 ± 0.013 | 0.048 ± 0.003 | 12.4 ± 0.1 |
| | 100 | 0.177 ± 0.015 | 0.035 ± 0.003 | 11.3 ± 0.2 |
| high salinity | | 0.133 ± 0.018 | 0.072 ± 0.008 | 29.1 ± 0.1 |
| | 100 | 0.251 ± 0.024 | 0.048 ± 0.003 | 10.8 ± 0.37 |
| connate brine | | 0.060 ± 0.002 | 0.056 ± 0.001 | 43.1 ± 0.3 |
| | 100 | 0.198 ± 0.009 | 0.036 ± 0.002 | 10.4 ± 0.3 |

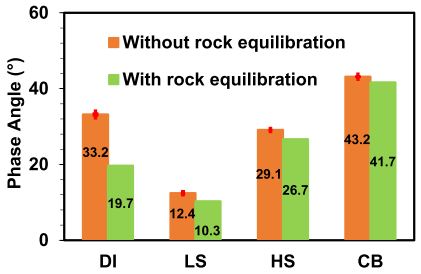


Figure 2. Phase angle (°) from interfacial viscoelasticity measurements of the crude oil and various aqueous phases without rock equilibration (orange) and with rock equilibration (green): deionized water (DI), low salinity (LS), high salinity (HS), and connate brine (CB).

Table 4. Elastic Modulus, Viscous Modulus, and Phase Angle: Brine Is Equilibrated with the Rock

| brine type | elastic modulus (mN/m) | viscous modulus (mN/m) | phase angle (°) |
|---|---|---|---|
| deionized water | 0.170 ± 0.018 | 0.056 ± 0.004 | 19.6 ± 0.5 |
| low salinity | 0.200 | 0.030 | 10.3 |
| high salinity | 0.100 | 0.040 | 26.7 |
| connate brine | 0.050 | 0.040 | 41.7 |

Table 5. Water−Oil Interfacial Tension Measurements

| | water−oil interfacial tension (mN/m) | |
|---|---|---|
| aqueous phase | without DEM | with 100 ppm DEM |
| deionized water | 10.4 ± 0.2 | 3.5 ± 0.2 |
| low-salinity brine | 7.5 ± 0.1 | 3.0 ± 0.1 |
| high-salinity brine | 5.6 ± 0.1 | 2.4 ± 0.1 |

Table 6. Water−Oil Contact Angle Measurements

| | water−oil contact angle (°) | |
|---|---|---|
| aqueous phase | without DEM | with 100 ppm DEM |
| deionized water | 53.6 ± 0.2 | 46 ± 1.1 |
| high-salinity brine | 63.7 ± 0.7 | 61.9 ± 0.1 |
| connate brine | 98.9 ± 0.2 | 78.7 ± 0.8 |

**Coreflow.** Table 7 lists the pore volume (PV), porosity ($\phi$), permeability measured by deionized water ($k_w$), initial water saturation ($S_{wi}$), and original oil-in-place (OOIP) of the cores in the four tests. It also includes capillary numbers for the tests, which are defined as the ratio of viscous to capillary forces [$N_c = (v\mu)/\sigma$, where $N_c$ is the capillary number, $v$ is Darcy velocity, $\mu$ is the viscosity, and $\sigma$ is the interfacial tension].

In tests 1, 3, and 4, HS, LS, and DI water are injected to around 2 PV, until there is no significant oil production. Next, 100 ppm DEM is dissolved in the injection water and the additional oil recovery due to DEM is recorded. In test 2, 100 ppm DEM is dissolved in HS brine from the beginning of the run to examine the efficiency of DEM in oil recovery compared to HS brine alone. The capillary numbers for tests 1, 3, and 4 in Table 7 are for secondary coreflooding, not accounting for the tertiary coreflooding with DEM.

Oil recovery with respect to original oil in place (OOIP) for the four tests is illustrated in Figure 3. Until 2 PV injection, test 1 has the lowest recovery of 58%. In comparison, injection of LS brine (test 3) and HS brine with 100 ppm DEM (test 2) is found to improve the oil recovery by about 21 and 22%, respectively. Test 4, with deionized water injection, has an intermediate recovery of about 63%. Interestingly, the oil

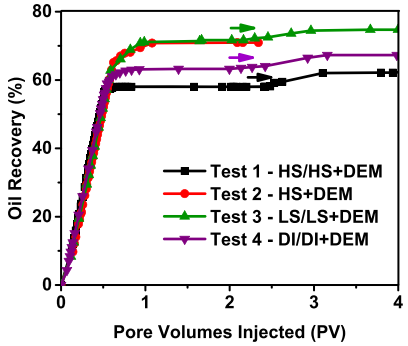


Figure 3. Oil recovery performance at injection rate of 2 PV/day. For tests 1, 3, and 4, arrows represent the change from the secondary to tertiary mode.

Table 7. Relevant Core Parameters for Coreflow[a]

| test no. | injection fluid | PV (mL) | $\phi$ (%) | $k_w$ (mD) | $S_{wi}$ (%) | OOIP (mL) | capillary number |
|---|---|---|---|---|---|---|---|
| 1 | HS/HS-DEM | 44.5 | 25.6 | 12.9 | 16.9 | 36.9 | $1.6 \times 10^{-07}$ |
| 2 | HS-DEM | 44.0 | 25.3 | 12.8 | 15.9 | 37.1 | $3.8 \times 10^{-07}$ |
| 3 | LS/LS-DEM | 44.0 | 25.3 | 12.0 | 18.2 | 36.4 | $1.2 \times 10^{-07}$ |
| 4 | DI/DI-DEM | 44.5 | 25.6 | 12.9 | 16.9 | 36.9 | $1.2 \times 10^{-07}$ |

[a]PV, pore volume; $\phi$, porosity; $k_w$, permeability measured with deionized water; $S_{wi}$, initial water saturation; OOIP, original oil in place


https://dx.doi.org/10.1021/acs.langmuir.0c01752
Langmuir 2020, 36, 12160−12167

recovery results are in line with the viscoelasticity measurements (Figure 2): the more elastic the oil−water interface, the higher the oil recovery. Based on the results of Figures 2 and 3, we suggest that for a given carbonate rock and different oils, we can expect the highest recovery from the highest interface elasticity. Therefore, in our study, interface viscoelasticity is a measure of oil recovery from injection of water in the cores.

In tests 1, 3, and 4, the effect of DEM at the tertiary stage is analyzed by adding 100 ppm DEM to the injection water after 2 PV injection. There is a slight increase in oil recovery; the effect of the surfactant is not significant in the tertiary stage (test 2).

Pressure drop plots for the four coreflow tests are presented in Figure 4. Generally, when there is emulsion formation, the pressure drop is high. There is also a higher pressure drop often in early period of water injection in a more water-wetting state. A third consideration in pressure drop is related to the elasticity of the water−oil interface. A more elastic interface reduces snap off, and therefore, a lower pressure drop should be expected compared to a lower elastic interface. A comparison of pressure drops in tests 1 and 2 (both high-salinity water injection) on the basis of interface elasticity agrees with the expected behavior. The test at LS injection (test 3) because of significantly higher interface elasticity compared to high-salinity water injection in test 1 gives a lower pressure drop, which is the expected behavior. Test 4 (DI water injection) results in a pressure drop between tests 1 and 3. This is not the case in early part, but the expected behavior is observed in the later stages of PV injection.

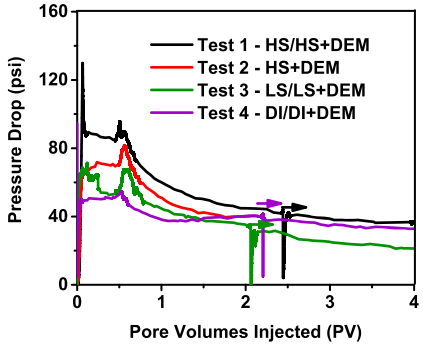


**Figure 4.** Pressure drop profiles of the coreflow tests. For tests 1, 3, and 4, arrows represent the change from the secondary to tertiary mode.

**Adsorption Measurements.** The absorbance spectra of DEM in high-salinity brine are presented in Figure 5. From these spectra, the calibration plot for the concentration of DEM in brine is prepared (Figure 6). As can be seen from the calibration plot in Figure 6, a linear trend of absorbance with respect to DEM concentration is attained by using the absorbance data at 230 nm.

To assess the adsorption of DEM onto the rock surface during water injection, a separate coreflow experiment is conducted by first saturating and aging the core with HS brine and then injecting 20 PV of HS brine mixed with 100 ppm DEM at a flow rate of 5 PV/day. In coreflow experiments, the DEM concentration in the produced brine initially drops to about 80 ppm, then increases steadily, and ultimately stabilizes at almost 100 ppm concentration after injection of 14 PV. This indicates a very low adsorption of the chemical onto the rock surface. A steady and constant permeability is maintained throughout the flow, as indicated by the pressure drop profile in Figure 7.

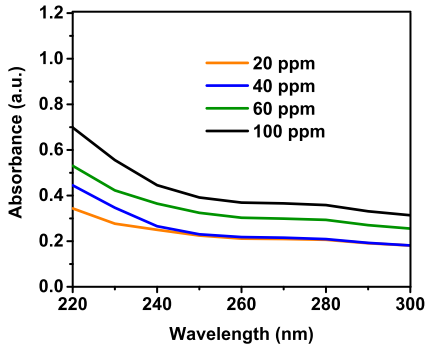


**Figure 5.** Absorbance spectra at different DEM concentrations in high-salinity brine.

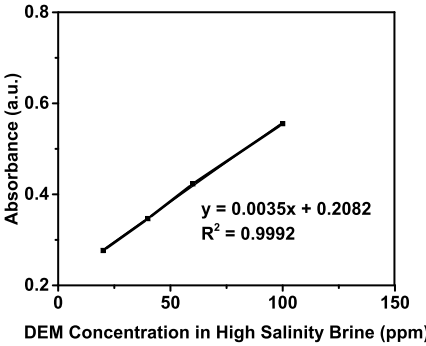


**Figure 6.** Calibration plot of DEM concentration in high-salinity brine based on absorbance data at 230 nm from Figure 5.

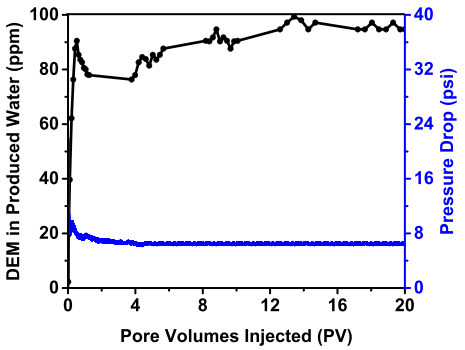


**Figure 7.** Pressure drop profile during dynamic adsorption coreflow and concentration of DEM in the produced water at the core outlet. The concentration of DEM at the core inlet is 100 ppm.

**Proposed Mechanism.** Based on our results, we propose the schematic in Figure 8 to describe the proposed mechanism in a simple way. When there is no added surfactant, only surface-active components in the oil adsorb to the interface. Depending on the salinity of water, asphaltenes are driven weakly or strongly to the interface, showing a difference in viscoelasticity. At sufficiently low interface elasticity, there is higher probability of crude oil front to breakdown during waterflooding, causing earlier breakthrough and higher isolated residual oil drops in the rock. When surfactants are added, they saturate the interface rapidly, forming structures with asphaltenes already at the interface. The surfactant network at the water−oil interface promotes interface elasticity. A


https://dx.doi.org/10.1021/acs.langmuir.0c01752
Langmuir 2020, 36, 12160−12167

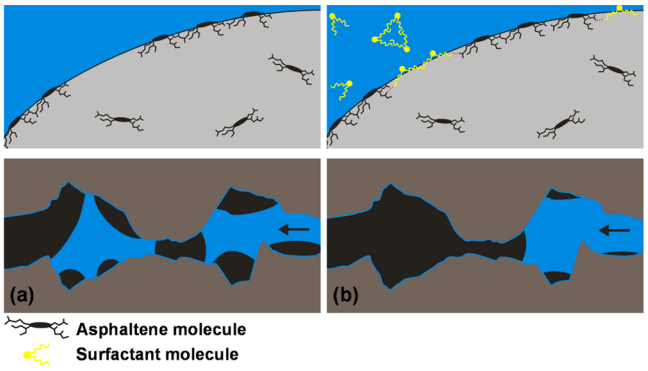


**Figure 8.** Schematic diagram showing the effect of crude oil−water interfacial viscoelasticity on IOR for (a) no added surfactants in the aqueous phase and (b) with added surfactants in the aqueous phase. The top image shows the molecular level interaction, and the bottom image represents the flow of oil in porous media.

higher interface elasticity results in a smoother oil flow during water oil displacement, increasing the oil recovery.

## CONCLUDING REMARKS

The oil recovery is comparable in coreflow from LSW injection and from 100 ppm DEM in HSW injection for the oil in this study. In our previous work,[17] when the oil recovery from LSW injection does not increase much beyond HSW injection, the addition of 100 ppm DEM to HSW gave higher recovery than LSW injection. The 100 ppm DEM is advantageous over LS water injection due to simplicity of the process and cost considerations.

The following main conclusions are drawn from this work.

1. The effect of salt concentration in the injected water on oil recovery may not be monotonic. The oil recovery without salt in the injected water is lower than that from a salt concentration of 0.1 wt %. At a salt concentration of 4 wt % in the injected water, the recovery is substantially less than that at 0.1 wt %.
2. Addition of 100 ppm DEM to the injected brine significantly increases the interface elasticity. The increase in elasticity is not pronounced by salt concentration in a range of 0−28 wt %.
3. There is a surprising close correlation between the oil recovery and interfacial elasticity.
4. Adsorption of the surfactant onto the rock surface is low. The low adsorption on the rock surface and preference for accumulation at the fluid−fluid interface allow an ultralow concentration of 100 ppm to be effective.
5. Interfacial viscoelasticity at very low salt concentrations should be conducted from the aqueous phase equilibrated with the rock.
6. In a simple interpretation, we can divide surfactants into two groups. In one group, they form structures such as micelles in the bulk phase and accumulate at the fluid−fluid interface without forming structures. The accumulation lowers the interfacial tension, which is proportional to the amount. In another group where the solubility in the bulk aqueous phase is low, they form structures in the bulk as well as structures at the interface. The non-ionic surfactant used in this work forms structures at the interface. The result is a significant effect on interface elasticity.

## AUTHOR INFORMATION


### Corresponding Author

**Abbas Firoozabadi** − *Reservoir Engineering Research Institute, Palo Alto, California 94301, United States; Department of Chemical and Biomolecular Engineering, Rice University, Houston, Texas 77005, United States;* orcid.org/0000-0001-6102-9534; Email: Abbas.Firoozabadi@Rice.edu

### Authors

**Taniya Kar** − *Reservoir Engineering Research Institute, Palo Alto, California 94301, United States*

**Tomás-Eduardo Chávez-Miyauchi** − *Universidad La Salle México, Mexico City 06140, Mexico*

**Mayur Pal** − *North Oil Company, Doha, Qatar*

Complete contact information is available at: https://pubs.acs.org/10.1021/acs.langmuir.0c01752


### Author Contributions

T.K. performed most of the experimental work and analysis. She wrote the first draft of the manuscript. T.-E.C.-M. did the initial part of the experiments and helped with ideas throughout the work. A.F. was the principal investigator and led the research. He shaped the manuscript. M.P. helped with ideas throughout the work.

### Notes

The authors declare no competing financial interest.

## ACKNOWLEDGMENTS

We thank the North Oil Company, Qatar, for all the help and financial support throughout the work.

## ABBREVIATIONS

IOR; improved oil recovery; ppm; parts per million; LSW; low-salinity waterflooding; IFT; interfacial tension; TBN; total base number; DI; deionized; TAN; total acid number; CMC; critical micelle concentration; PV; pore volume; DCM; dichloromethane; LS; low salinity; HS; high salinity; CB; connate brine; OOIP; original oil in place

## REFERENCES


(1) Tang, G. Q.; Morrow, N. R. Salinity, temperature, oil composition, and oil recovery by waterflooding. *SPE Reservoir Eng.* **1997**, *12*, 269−276.

(2) Dang, C.; Nghiem, L.; Fedutenko, E.; Gorucu, E.; Yang, C.; Mirzabozorg, A. Application of artificial intelligence for mechanistic modeling and probabilistic forecasting of hybrid low salinity chemical flooding. In *SPE Annual Technical Conference and Exhibition;* Society of Petroleum Engineers 2018.

(3) Yousef, A. A.; Al-Saleh, S. H.; Al-Kaabi, A.; et al. Laboratory investigation of the impact of injection-water salinity and ionic content on oil recovery from carbonate reservoirs. *SPE Reservoir Eval. Eng.* **2011**, *14*, 578−593.

(4) Myint, P. C.; Firoozabadi, A. Thin liquid films in improved oil recovery from low-salinity brine. *Curr. Opin. Colloid Interface Sci.* **2015**, *20*, 105−114.

(5) Bartels, W. B.; Mahani, H.; Berg, S.; et al. Literature review of low salinity waterflooding from a length and time scale perspective. *Fuel* **2019**, *236*, 338−353.

(6) Lee, S. Y.; Webb, K. J.; Collins, R. et al. Low salinity oil recovery−increasing understanding of the underlying mechanisms of double layer expansion, *In IOR 2011-16th European Symposium on Improved Oil Recovery*; European Association of Geoscientists & Engineers 2011.

(7) Lu, Y.; Najafabadi, N. F.; Firoozabadi, A. Effect of temperature on wettability of oil/brine/rock system. *Energy Fuels* **2017**, *31*, 4989−4995.
(8) Anderson, W. G. Wettability literature survey-Part 1: Rock/oil/brine interactions and the effects of core handling on wettability. *J. Petrol. Technol.* **1986**, *38*, 1−1144.
(9) Austad, T.; Shariatpanahi, S. F.; Strand, S.; et al. Conditions for a low-salinity enhanced oil recovery (EOR) effect in carbonate oil reservoirs. *Energy Fuels* **2011**, *26*, 569−575.
(10) Zahid, A.; Stenby, E. H.; Shapiro, A. A. Improved oil recovery in chalk: Wettability alteration or something else? In *SPE Europec/EAGE Annual Conference and Exhibition;* Society of Petroleum Engineers 2010.
(11) Nasralla, R. A.; Alotaibi, M. B.; Nasr-El-Din, H. A. Efficiency of oil recovery by low salinity water flooding in sandstone reservoirs. In *SPE Western North American Region Meeting*; Society of Petroleum Engineers 2011.
(12) Li, Y. Oil recovery by low salinity water injection into a reservoir: A new study of tertiary oil recovery mechanism. *Transp. Porous Media* **2011**, *90*, 333−362.
(13) Shehata, A. M.; Alotaibi, M. B.; Nasr-El-Din, H. A. Waterflooding in carbonate reservoirs: Does the salinity matter? *SPE Reservoir Eval. Eng.* **2014**, *17*, 304−313.
(14) Pal, M.; Tarsauliya, G.; Patil, P. et al. Dreaming big ″Surfactant injection in a giant offshore carbonate field″, from successful injection trials to pilot design and implementation, *In IOR 2019−20th European Symposium on Improved Oil Recovery*; European Association of Geoscientists & Engineers 2019.
(15) Uren, L. C.; Fahmy, E. H. Factors influencing the recovery of petroleum from unconsolidated sands by waterflooding. *Trans. AIME* **1927**, *77*, 318−335.
(16) Chávez-Miyauchi, T. E.; Firoozabadi, A.; Fuller, G. G. Nonmonotonic elasticity of the crude oil−brine interface in relation to improved oil recovery. *Langmuir* **2016**, *32*, 2192−2198.
(17) Cho, H.; Kar, T.; Firoozabadi, A. Effect of interface elasticity on improved oil recovery in a carbonate rock from low salinity and ultra-low concentration demulsifier. *Fuel* **2020**, *270*, 117504.
(18) Lucassen-Reynders, E. H. Interfacial viscoelasticity in emulsions and foams. *Food Struct.* **1993**, *12*, 1.
(19) Fuller, G. G. Rheology of mobile interfaces. *Rheol. Rev.* **2003**, 77−124.
(20) Van den Tempel, M. Surface rheology. *J. Non-Newtonian Fluid Mech.* **1977**, *2*, 205−219.
(21) Freer, E. M.; Svitova, T.; Radke, C. J. The role of interfacial rheology in reservoir mixed wettability. *J. Petrol. Sci. Eng.* **2003**, *39*, 137−158.
(22) Fan, Y.; Simon, S.; Sjöblom, J. Interfacial shear rheology of asphaltenes at oil−water interface and its relation to emulsion stability: Influence of concentration, solvent aromaticity and nonionic surfactant. *Colloids Surf., A* **2010**, *366*, 120−128.
(23) Pradilla, D.; Simon, S.; Sjöblom, J. Mixed interfaces of asphaltenes and model demulsifiers, part II: Study of desorption mechanisms at liquid/liquid interfaces. *Energy Fuels* **2015**, *29*, 5507−5518.
(24) Bidhendi, M. M.; Garcia-Olvera, G.; Morin, B. Interfacial viscoelasticity of crude oil/brine: an alternative enhanced-oil-recovery mechanism in smart waterflooding. *SPE Journal* **2018**, *23*, 803−818 SPE-169127-PA..
(25) Reilly, T.; Medina, B.; Lehmann, T. et al. Select naphthenic acids beneficially impact oil-water dynamics during smart water-flooding, *In SPE Annual Technical Conference and Exhibition*; Society of Petroleum Engineers 2018.
(26) Alvarado, V.; Moradi Bidhendi, M.; Garcia-Olvera, G. et al. Interfacial visco-elasticity of crude oil-brine: An alternative EOR mechanism in smart waterflooding, *In SPE Improved Oil Recovery Symposium*; Society of Petroleum Engineers 2014.
(27) Emadi, A.; Sohrabi, M. Visual investigation of oil recovery by low salinity water injection: formation of water micro-dispersions and wettability alteration, In *SPE Annual Technical Conference and Exhibition*; Society of Petroleum Engineers 2013.
(28) Garcia-Olvera, G.; Alvarado, V. The potential of sulfate as optimizer of crude oil-water interfacial rheology to increase oil recovery during smart water injection in carbonates, *In SPE Improved Oil Recovery Conference*; Society of Petroleum Engineers 2016.
(29) Chávez-Miyauch, T. E.; Lu, Y.; Firoozabadi, A. Low salinity water injection in Berea sandstone: Effect of wettability, interface elasticity, and acid and base functionalities. *Fuel* **2020**, *263*, 116572.
(30) Sun, M.; Mogensen, K.; Bennetzen, M.; Firoozabadi, A. Demulsifier in injected water for improved recovery of crudes that form water/oil emulsions. *SPE Res. Eval. Eng.* **2016**, *19*, 1−672.
(31) Stalder, A. F.; Kulik, G.; Sage, D.; et al. A snake-based approach to accurate determination of both contact points and contact angles. *Colloids Surf., A* **2006**, *286*, 92−103.
(32) Stalder, A. F.; Melchior, T.; Müller, M.; et al. Low-bond axisymmetric drop shape analysis for surface tension and contact angle measurements of sessile drops. *Colloids Surf., A* **2010**, *364*, 72−81.
(33) Aslan, S.; Najafabadi, N. F.; Firoozabadi, A. Non-monotonicity of the contact angle from NaCl and $MgCl_2$ concentrations in two petroleum fluids on atomistically smooth surfaces. *Energy Fuels* **2016**, *30*, 2858−2864.
(34) Brooks, C. F.; Fuller, G. G.; Frank, C. W.; et al. An interfacial stress rheometer to study rheological transitions in monolayers at the air− water interface. *Langmuir* **1999**, *15*, 2450−2459.


https://dx.doi.org/10.1021/acs.langmuir.0c01752
*Langmuir* 2020, 36, 12160−12167